

TECHNICAL MEMORANDUMS  
NATIONAL ADVISORY COMMITTEE FOR AERONAUTICS

No. 601

WRINKLING PHENOMENA OF THIN FLAT PLATES  
SUBJECTED TO SHEAR STRESSES

By F. Bollenrath

From Luftfahrtforschung, Vol. VI, No. 1, December 12, 1929

REPORT OF INVESTIGATION

PERFORMED AT THE NATIONAL ADVISORY COMMITTEE FOR AERONAUTICS

WASHINGTON, D. C.

DECEMBER 12, 1929

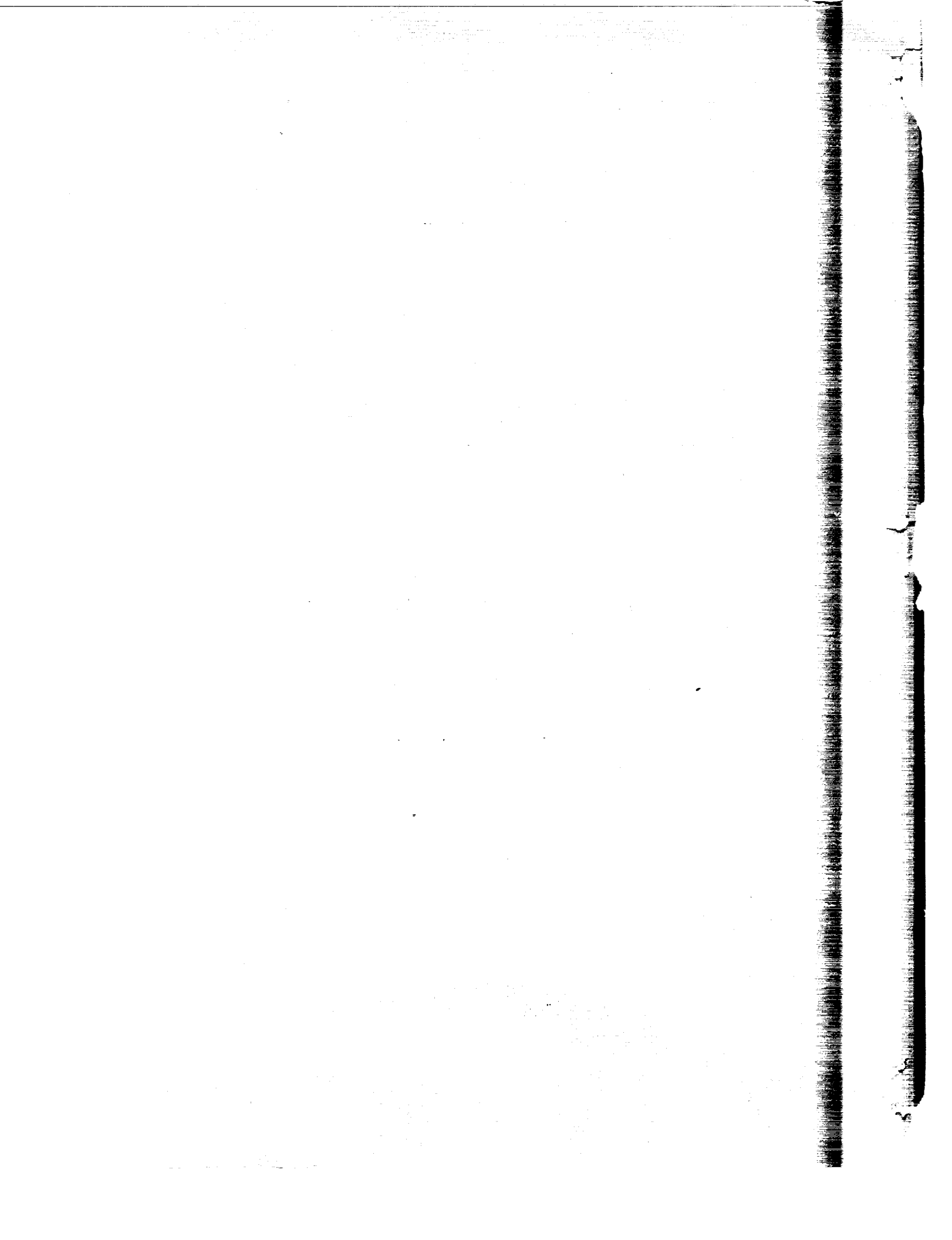
RESEARCH REPORT

NATIONAL ADVISORY COMMITTEE FOR AERONAUTICS

WASHINGTON, D. C.

Washington  
January, 1931

FILE COPY  
National Advisory Committee  
for Aeronautics  
Washington, D. C.



NATIONAL ADVISORY COMMITTEE FOR AERONAUTICS

---

TECHNICAL MEMORANDUM NO. 601

---

WRINKLING PHENOMENA OF THIN FLAT PLATES

SUBJECTED TO SHEAR STRESSES\*

By F. Bollenrath

The present report covers a series of tests on thin, flat elastic strips restrained at two parallel edges and subjected to shear by conversely directed stresses. The stress is uniformly distributed over the constrained edges and acts in the plane of the strip. As soon as the shear in such strips exceeds a certain limit the equilibrium between the applied and the internal stresses is interrupted and instability prevails. Now, if the wall is thin with respect to the width of the median plane of the body, the incipient instability is attended by a characteristic flexural phenomenon which appears as a pronounced lobe or wrinkle. Thus, Figure 10 shows two restrained duralumin plates where the type of shear just mentioned, resulted in a wavelike lobe. The deflection in these plates is so pronounced as to remain visible when the load had been relieved.

Knowledge of the conditions under which this wrinkling under shear (i.e., the shear producing instability) occurs, is of great import for many structural components, particularly in light metal structures. The problem treated here is applicable to all cases where a thin wall, through the type of its attachment

---

\*"Ausbeulerscheinungen an ebenen, auf Schub beanspruchten Platten." From Luftfahrtforschung, Vol. VI, No. 1, December 12, 1929.

to other parts, is intended to take up and transmit stresses, as in plate girders, bulkheads, fuselages and wings of various airplane types.

Two limiting cases (Fig. 1) for thin bodies stressed in shear are those of round plates and thin-walled tubing (Reference 17), the latter of which, however, really belongs to the "shell" group. The first experiments on this subject were made by Lord Rayleigh (Reference 14), who investigated the case of a vibrating system with reference to its natural frequency of vibration. Bryan (Reference 3), Walter Ritz (Reference 15), and S. Timoschenko (References 21 and 22) based their experiments on the stability equations of an elastic plate for defining its buckling stresses.\*

In the following we describe the development of the calculation of this problem from approximation to exact solution.

Let  $E$  = Young's modulus ( $\text{kg}/\text{cm}^2$ ),  
 $m$  = transverse elongation factor (Poisson's ratio),  
 $\mu = 1/m$ ,  
 $L$  = length of rectangular plate (cm)  
 $h$  = thickness of plate (cm),  
 $a$  = width of plate (cm),  
 $u, v, w$  = displacements in the direction of  
           $x, y$ , and  $z$  axes

---

\*St. Bergmann and H. Reissner reported on the appearance of instability in corrugated plates under shear in "Neuere Probleme aus der Flugzeugstatik," and "Über die Knickung von Wellblechstreifen bei Schubbeanspruchung." Zeitschrift für Flugtechnik und Motorluftschiffahrt, No. 18, 1929, pp. 475-481.

$s$  = shear per unit of length in restrained edge (kg/cm),

$p$  = compression per unit of edge surface parallel to  $x$  axis (kg/cm<sup>2</sup>),

$q$  = tension per unit of edge surface parallel to  $y$  axis (kg/cm<sup>2</sup>),

$r$  =  $p/q$ ,

$q_e$  = Euler's buckling load for a strip of length  $a$ , thickness  $h$ , and width  $1$  (kg/cm<sup>2</sup>),

$\lambda$  = wave length parallel to the restrained edges,

$D = \frac{E h^3}{12 (1-\mu^2)}$  flexural rigidity,

$A = \frac{a^2 s}{D}$ .

#### Wrinkling Due to Shear (W. E. Lilly's method)

Lilly (References 10, 11, and 12) in his work on wrinkling of plate girders, applied the well-known strip method. Thus, we see in Figure 2, the wavelike deflection of the median plane of a plate under shear after exceeding the shear strength, expressed as lines of equal deflection perpendicular to the median plane. The figures attached to the contours have a relative significance only. We can visualize the same deformation as having been induced by tension and compression stresses of the kind shown in Figure 2, and which are dimensioned in magnitude and direction so as to balance a shear stress of the intended type in magnitude and direction. The applicability of Lilly's method of approximation rests on this theorem. He con-

siders, according to Figure 3, one single panel - between two stiffeners - of a web member collapsed in the form of a half-wave. The line o-o denotes the center line of the half-wave. Such panel then is stressed in tension and compression as a constrained rectangular plate of length  $L$  and width  $\lambda/2$  (See Fig. 4).

Now when we divide the plate in strips b-b perpendicular to each other, parallel to axis  $x$  and a-a, and parallel to axis  $y$ , strip a-a is stressed in bending and compression, and strip b-b in tension and bending. So when we assume a sinuous deformation and apply Euler's formulas for the buckling load we find

$$p \left( \frac{4}{\lambda^2} - \frac{1}{r L^2} \right) = \pi^2 \frac{E h^2}{12} \left( \frac{16}{\lambda^4} + \frac{1}{L^4} \right) \quad (1)$$

There is a minimum for equation (1) when

$$\frac{\lambda^2}{4 L^2} = \frac{\sqrt{r^2 + 1} - 1}{r} \quad (2)$$

This formula (2) shows that the wave length is not affected by the plate width; it merely depends on  $L$  and  $r$ . Formula (1) in connection with the  $\lambda$  values of formula (2) yields

$$p = \frac{3 \pi^2 E h^2}{3 \lambda^2} = \frac{\pi^2 E h^2}{12 L^2} \frac{2 r}{\sqrt{r^2 + 1} - 1} \quad (3)$$

If, by  $L = \lambda/2$ , the wave runs at  $45^\circ$  to the constrained edges, the stress is a pure shear stress for  $r = 1$ . In that case, formula (2) yields

$$\lambda^2 = 4 (\sqrt{3} - 1) L^2 = 1.64 L^2 \quad (4)$$

According to these formulas the applicability of such calculations is contingent on the condition that the dimensions of the plate allow the formation of a half-wave only.

Wrinkling Due to Shear (S. Timoschenko's method)  
(Reference 22)

This approximation method is based on the potential energy of the system (Reference 21). The appearance of the unstable equilibrium attitude becomes evident as a potential energy in bending  $V$ , when deflecting from the plane, and as a lower potential energy in shear  $V_1$ , so that

$$V = V_1. \quad (5)$$

Starting with a rectangular, all-around supported plate, the length-width ratio  $L/a$  is progressively increased and soon reaches a limit value, valid for the infinitely long plate strip; the type of support of the smaller sides becomes secondary. In this manner the formula for the wrinkling of a long plate from the median plane  $w$  becomes:

$$w = A \sin \pi \frac{y}{b} \sin \pi \frac{\lambda}{2} (x - a y) \quad (6)$$

and for wrinkling due to shear

$$\tau = \frac{\sigma_e}{2\alpha} \left[ 6 \alpha^2 + 2 + \frac{\lambda^2}{4 \alpha^2} + \frac{4 b^2}{\lambda^2} (1 + \alpha^2)^2 \right] \quad (7)$$

For a minimum  $\tau$  we have:

$$\frac{\lambda}{2} = a \sqrt{1 + \alpha^2} \quad (8)$$

$$\alpha = \frac{1}{\sqrt{2}} \quad (9)$$

so that

$$\tau = c \sigma_e \quad (10)$$

Figure 5 shows the  $c$  values for various relations of plate length  $L$  to plate width  $a$ . It will be noted that  $c$  soon approaches the value for  $L/a = \infty$ .

#### Wrinkling Due to Shear (R. V. Southwell and Sylvia W. Skan)

These authors give a strict solution (References 18 and 19) for the case of a flat elastic strip of infinite length. But the distribution of stresses in a thin plate over an infinitely small plate element is without any practical significance, according to Love. For that reason we represent the stresses applying at the edges by their resultants and their resultant moments with respect to the unit length of the border line, i.e., the curve in which the edge passes through the median plane. Now according to St. Venant's theorem the effects of two systems of stresses yielding identical resultants and resultant moments are practically identical at some distance from the edge.

Selecting from Figure 6 a plate element  $dx$  long and  $dy$  wide, we have, since the stress in a plate depends on the shape of the elastic surface:

1. On the edges parallel to the x axis - bending stresses linearly increasing with the distance from the median plane, statically equivalent to a force couple with moment  $G_2$ ; torsional stresses equivalent to a torsion moment  $H_1$ ; shear stresses in the direction of the z axis with resultant  $N_2$ ; shear stresses in the direction of the x axis with resultant  $S$ .

2. On the edges parallel to the y axis - bending stresses linearly increasing with the distance from the median plane, statically equivalent to a couple of moment  $G_1$ ; torsion stresses equivalent to a torsion moment  $H_1$ ; shear stresses in the direction of the z axis with resultant  $N_1$ ; shear stresses in the direction of the y axis with resultant  $S$ .

Now the equilibrium equations applied to the deformed plate in Figure 7 are as follows:

$$\left. \begin{aligned} \frac{\partial N_1}{\partial x} + \frac{\partial N_2}{\partial y} &= -2S \frac{\partial^2 w}{\partial x \partial y} \\ \frac{\partial G_1}{\partial x} - \frac{\partial H_1}{\partial y} - N_1 &= 0 \\ \frac{\partial H_1}{\partial x} - \frac{\partial G_2}{\partial y} + N_2 &= 0 \end{aligned} \right\} \quad (11)$$

$$\left. \begin{aligned} \frac{\partial^2 G_1}{\partial x^2} - \frac{\partial^2 H_1}{\partial y \partial x} - \frac{\partial N_1}{\partial x} &= 0 \\ \frac{\partial^2 H_1}{\partial x \partial y} - \frac{\partial^2 G_2}{\partial y^2} + \frac{\partial N_2}{\partial y} &= 0 \\ - \frac{\partial^2 G_1}{\partial x^2} + \frac{2 \partial^2 H_1}{\partial x \partial y} - \frac{\partial^2 G_2}{\partial y^2} + 2 S \frac{\partial^2 w}{\partial x \partial y} &= 0 \end{aligned} \right\} \quad (12)$$

The stress resultants and the resultant stress moments are combined to read:

$$\left. \begin{aligned} G_1 &= -D \left( \frac{\partial^2 w}{\partial x^2} + \mu \frac{\partial^2 w}{\partial y^2} \right) \\ G_2 &= -D \left( \frac{\partial^2 w}{\partial y^2} + \mu \frac{\partial^2 w}{\partial x^2} \right) \\ H_1 &= D (1 - \mu) \frac{\partial^2 w}{\partial x \partial y} \end{aligned} \right\} \quad (13)$$

This, together with the above formulas, yields

$$\begin{aligned} D \left( \frac{\partial^4 w}{\partial x^4} + \mu \frac{\partial^4 w}{\partial x^2 \partial y^2} + 2 (1 - \mu) \frac{\partial^4 w}{\partial x^2 \partial y^2} + \right. \\ \left. + \frac{\partial^4 w}{\partial y^4} + \mu \frac{\partial^4 w}{\partial x^2 \partial y^2} \right) = - 2 S \frac{\partial^2 w}{\partial x \partial y} \end{aligned} \quad (14)$$

$$D \left( \frac{\partial^4 w}{\partial x^4} + 2 \frac{\partial^4 w}{\partial x^2 \partial y^2} + \frac{\partial^4 w}{\partial y^4} \right) = - 2 S \frac{\partial^2 w}{\partial x \partial y} \quad (15)$$

$$D \Delta \Delta w + 2 S \frac{\partial^2 w}{\partial x \partial y} = 0 \quad (16)$$

Southwell resolved this last equation (16). Writing

$$w = Y e^{i \kappa x}, \quad (i = \sqrt{-1}) \quad (17)$$

formula (16) becomes

$$Y^{(4)} - 2 \kappa^2 Y'' + 2 i \kappa S Y' + \kappa^4 Y = 0 \quad (18)$$

for function  $Y(y)$ , and must be integrated for the limiting equations

$$y = \pm \frac{a}{2}, \quad Y = Y' = 0. \quad (19)$$

Finally

$$Y = e^{i\lambda y} \quad (20)$$

yields for  $\lambda$  an equation of the fourth degree, whose four roots give the solution. According to this solution the median plane of the plate deflects, due to exceeding the shear strength, into a uniformly lobed surface. The lowest shear strength is

$$s = 88.7 \frac{D}{a^2} \text{ kg/cm} \quad (21)$$

and the conformal wave length

$$\lambda = 1.6 a \quad (22)$$

This length is contingent on the plate width, as shown by formula (2). Thus Figure 8 presents the wrinkles due to shear plotted against the ratio: wave length/plate width, according to Southwell and Skan. The curve of the first solution is expedient for the case of deforming into one, the curve of the second solution into two rows of half-waves in the direction of the plate width. Accordingly, a plate under simple shear, whose stiffeners bring about two rows of half-waves in the direction of the plate width, is more conducive to higher shear strength than one producing but one row.

## E x p e r i m e n t s

To produce a shear stress in a plate strip of the kind described, we developed a clamping arrangement which constrains the test strip on two parallel edges at a width of 5 mm between flat surfaces, as exhibited in Figure 9, where (a,a) are the test strips and (b,b) the two constraining clamps. The stresses acting along the constrained edges shifted the latter parallel to each other and put the strips under shear.

The loading was accomplished by applying a tension on the inside clamps, which is evenly distributed over both test strips and taken up by the outside clamps.

For the experiments on brass and duralumin we used a 5-ton tension machine (Fig. 10, vertical arrangement), and for the celluloid tests we adhered to the horizontal method (Coker) because of the small loads needed and the comparatively heavy weight of the clamping device.

The relative displacement of the constrained edges was measured with four Zeiss gauges (one division = 1/100 mm).

## Conditions of the Boundaries or Edges

The problem is whether and to what extent the conditions and assumptions upon which the calculations are based are complied with in these tests. Southwell and Skan analyze, for example, an infinitely long plate strip, a condition which is practically unrealizable. The strips used here are of limited length

and with free edges; consequently the problem is to discover what effect this substitution of finite strip length for one of infinite length relative to the stress distribution over the whole strip has on the magnitude of the shear stress and on the type of deformation. Then, another question to be answered is, the role played by the type of support of the smaller sides or of the ends of the strip.

Professor E. G. Coker (Reference 5) reports on his optical experiments with transparent bodies subjected to shear. He defines the stress distribution along a line  $O X$  (Fig. 12). The boundary conditions for the plates are: The long sides are constrained and are shifted parallel in the plane of the plate; the short sides are free. Some of his results are indicated in Figure 13. The origin of the coordinates is in the center of  $O X$ . The plate lengths (in inches) are the abscissas and the stresses (in pounds per square-inch) are the ordinates. The data in Figure 13 are for a plate 2 inches wide. According to his tests the shear distribution in a rectangular plate is parabolic along  $O X$  (curve a in Fig. 13). When the ratio of  $a$  to  $L$  decreased the curve of the stress distribution first flattened out at the tip (curves b and c, Fig. 13). For still smaller  $A/L$  ratios, local raises in stress distribution occurred near the free edges (point 1 on curve d and point 2 on curve e). In the middle of the strip the distribution was practically uniform.

Andrade (Reference 1) gives an experimental and analytical treatise of the problem. His tests were made on a 16" x 4" x 4" rectangle of gel, a glycerine-gelatine compound. The two long sides were nailed by thin copper screening to a board. Then the screening was heated and pressed on the gel-body. The deformation was produced by parallel shifting of the plates. For defining the displacement he applied the optical method of Charles Pearson and A. F. C. Pollard ("An Experimental Study of the Stresses in Masonry Dams, Drapers Company Research Memoirs, Technical Series II, V). Andrade observed the same local stress increases near the free edge, but his calculations do not agree with his experiments, a fact which prompted him to speak of the inadequacy of his applied analytical methods.

L. N. G. Filon (Reference 6) examined a beam of rectangular cross section which is stressed in shear applied to the upper and lower fibers. Here Coker's observations are strikingly confirmed.

E. Inglis (Reference 7) treats the same problem, but attacks it from a different angle and his results are in close agreement with Professor Coker's figures. Inglis based his calculation on the superposition of two cases. In the first case he constrains the plate (Fig. 14) at edges AB and CD, leaving AD and BC free. Then he subjects the edges to a uniform shear acting in the plane of the plate. In the other case, the plate AB,CD is so stressed in shear, which is uniformly distributed

over the four edges, that the shear at the edges AD and BC is in opposite direction to the shear of the first case. The result is an absence of shear on edges AD and BC.

The results of Inglis' experiments are exhibited in Figures 14-18. Figure 14, in particular, shows the distribution of shear along OX ( $y = 0$ ); the edges AB and CD are constrained, the shear is uniform over AD. In Figure 15, we note the shear perpendicular to boundary AB ( $y = 1$ ); it is uniformly distributed over AD, with AB and CD constrained. Figure 16 shows the almost parabolic distribution along OX ( $y = 0$ ) for a square plate; Figure 17, the shear along OX for a plate with ratio length - width = 2; and Figure 18, for ratio - length/width = 4. In the last figure the flatness of the shear curve is very noticeable. The effect of the free edge does not last beyond 1.5 times the plate width to plate center. In conformity with the tests of the author, the smallest ratio of plate length to plate width = 8.5, justifies our assumption that the stress distribution is practically uniform over the whole strip, and that the free edges have no material effect on the test data.

The experiments included tests with celluloid, duralumin and brass.

#### C e l l u l o i d

For the calculation of the deformations and of the wrinkles due to shear, it is absolutely essential to know the longitudinal and the transverse elongation factors. For this reason,

special stress was laid on the determination of these figures, which was accomplished by micrometric measurement of rectangular test plates with the Martens reflecting instruments. The length of the spring was 100 mm for the longitudinal, and 25 mm for the transverse elongation. By a distance of 1125 mm and a height of 4.5 mm, a 1/5000 gear ratio was obtained. The tests were made on the 10-ton Losenhausen machine in the Aerodynamic Institute of the technical high school at Aachen, which also included the use of the 1000-kilogram metering box.

Celluloid proved particularly suited to such experiments. The proportional elastic limit was reached at 180 kg/cm<sup>2</sup> tension and by a comparatively high total elongation of 0.6%. At failure the material showed a 7-10 per cent elasticity by a total elongation of 26 per cent.

We examined eight different kinds of celluloid, according to Table I. The stress strain curves in Figure 19 show the characteristic behavior of the celluloid until failure: an approximately even raise in elongation with the stresses up to the yield limit, above which the breakdown becomes very perceptible. There is a basic difference between the clear, transparent and the colored celluloid beyond the yield point. The colored material shows a marked drop in stress, followed by a subsequent raise. This is most likely due to the coloring matter.

The nature of celluloid to follow Hooke's law to the yield

point and then to enter a so-called plastic state, proved very fortunate in subsequent wrinkling tests. In these we used the plates 5-8 of Table I, which, with respect to modulus of elasticity ( $E = 15,800$  to  $23,300$  kg/cm<sup>2</sup>) and the transverse elongation ( $m = 2.415$  to  $2.8$ ) gave us more room for action.

TABLE I. Modulus of Elasticity of different Kinds of Celluloid

Number	Kind	E Modulus of elasticity kg/cm <sup>2</sup>	Transverse elongation m	Thickness h cm
1	clear	26,600	2.4	0.19
2	"	26,700	2.4	0.19
3	white	24,500	2.0	1.51
4	"	22,500	3.66	0.08
5	clear	28,000	2.45	0.052
6	"	16,000	2.8	0.05
7	"	22,500	2.56	0.05
8	white	23,300	2.45	0.031
9	clear	15,800	2.415	0.051

Particular attention was paid to temperature and humidity while making the tests.

#### T e s t   D a t a

a) Wrinkling stress.-- By a certain shear the constrained edges of a plate width  $a$  may be shifted parallel by an amount  $g'$ . Expressing  $a$  and  $b$  in centimeters, formula

$$g = \frac{g'}{a} 100\% \quad (23)$$

now is to denote the shifting of the plate width in per cent.

The behavior of the plate subjected to shear is analyzed in Figure 20, where the loading  $s$  (kg/cm is plotted against

the maximum deflection from plane  $w$  (in centimeters  $\cdot 10^{-5}$ ) and against displacement  $g$  (in per cent). The dimensions of the plate were: thickness,  $h = 0.05$  cm; width,  $a = 1.9$  cm; and length,  $L = 23.7$ . By critical shifting here when  $g = 0.8\%$  (point A), the load deflection line begins to deflect, the load increases progress more slowly than before by corresponding displacements. This incipient deflection of the load line is simultaneously accompanied by a deflection from the plane. But even before the deflection from the central plane assumed measurable significance, the incipient buckling became noticeable through the distorted image of the reflected plate.

A second test with a celluloid strip of thickness  $h = 0.05$  cm, and width  $a = 1.6$  cm, is illustrated on Figure 21. The load deflection line is straight to point A, which corresponds to a displacement  $g = 0.78\%$ , where a bend occurs. This means the proportional limit has been reached and exceeded. Above this bend the line continues almost linearly, except for the more pronounced slope toward the axis of displacement. But the second portion itself shows at B a sudden, stronger deflection toward the axis of displacement; the load stages for obtaining equivalent displacements as before, become materially smaller. Bulging sets in; the wrinkling shear has been reached. But it occurs in this case above the yield limit; the deflection is inelastic in contrast to Figure 20.

TABLE II. Tests 1-9

Material, Celluloid  
 Modulus of elasticity,  $E = 16,000 \text{ kg/cm}^2$   
 Poisson's ratio,  $m = 2.8$   
 Plate thickness,  $h = 0.05 \text{ cm}$

Test No.	Plate width a cm	a/h	Wrinkling load s kg/cm	Displacement %	$k'$	$k'$ mean	k	Wave length $\lambda$ cm	$\frac{\lambda}{a}$
1	1.9	38	2.635	0.600	76,900	76,600	50.0	4.16	2.18
2	1.9	38	2.635	0.643	76,900			4.20	2.18
3	1.8	36	2.945	0.667	76,300	Elas-		3.68	2.04
4	1.8	36	2.945	0.667	76,300	tic		3.69	2.05
5	1.7	34	3.31	0.824	76,500	defor-		3.25	1.9
6	1.7	34	3.31	0.848	76,500	mation		3.46	2.03
7	1.6	32	3.49	0.900	73,200			3.104	1.94
8	1.5	30	3.62	0.734	66,800			2.91	1.94
9	1.4	28	3.86	0.843	62,000			2.63	1.88

By observing the appearance of deflection above as well as below the limit of elastic displacements, we made a series of tests with celluloid and defined the wrinkling load (Test series Nos. 1-9, Table II).

We considered as wrinkling load that load at which the first sign of measurable deflection from the central plane was noted. Hereby it should be taken into consideration that the load at wrinkling will be about as high as point B in Figure 20, but even at that it will be 25% lower than the theoretical figure.

Thus the quality of the approximation to the theoretical buckling load remains to a certain extent a question of the constraint. The experimental values should prove useful for the designer, because they supply a practical criterion of incipient wrinkling, for the danger of collapse lies not so much in the

formation of wrinkles as in the material displacements and in the pronounced uneven plate stresses accompanying the inception of deflection.

The results of the first test series (tests 1-9) are given in Table II and Figure 22. The curve representing the dependence of the wrinkling load on  $a/h$  may be expressed in the form of the equation

$$s = k \frac{D}{a^2} \text{ kg/cm} \quad (23)$$

When  $a/h$  falls below a certain value the experimental wrinkling loads with decreasing  $a/h$  deviate more and more from those expected according to the preceding formula. The basis of this limited applicability is Euler's load formula. Back in 1845 E. Lamarle (Reference 9) pointed out that the proportional limit of Euler's formula in its original form was to be accepted as limit of validity. (Todhunter and Pearson, "A History of Elasticity and Strength of Materials," Vol. I, No. 1253 ff., Cambridge, 1886.) The unlimited validity of Euler's formula in a more general form was established by Engesser (Reference 3), and appeared in 1895 (Reference 4), the accuracy of which was later confirmed by v. Karman (Reference 8).

The proportional limit is exceeded whenever wrinkling occurs under a smaller load than could be expected according to formula  $s = k \frac{D}{a^2}$ . The correct relation between shifting and stress, upon which the calculation is based, exists no longer. As the  $a/h$  ratio becomes smaller the assumption of a "thin plate" loses in

identity. Expressing formula (23) as

$$k \frac{E}{1 - \mu^2} \frac{1}{12} = s \frac{a^2}{h^3} = k'$$

$k'$  remains, as long as the deflection occurs below the proportional limit for shear, an invariable as proved by tests 1-6. If, to arrive at wrinkling, the proportional limit is exceeded,  $k'$  becomes so much smaller as the permanent deformation is stronger at buckling. Consequently,  $k'$  yields  $k$  from the experimental values within the elastic range, which, according to tests 1-6, is  $k = 50$ .

Three other series of tests on celluloid, Nos. 8, 9, and 10, Table I) - tests Nos. 10 to 16, 17 to 26, and 27 to 36 yield practically the same data, and are exhibited in Tables III, IV, and V, and Figure 22.  $k = 51$ , 52, and 49.3. The transition from elastic to inelastic deflection is characterized by  $a/h = 34$ , 32.2 to 35.5 and 31.4 to 29.4.

TABLE III. Tests 10-16

Material, Celluloid  
 Modulus of elasticity,  $E = 22,500 \text{ kg/cm}^2$   
 Poisson's ratio,  $m = 2.56$   
 Plate thickness,  $h = 0.05 \text{ cm}$

Test No.	Plate width a cm	a/h	Wrinkling load s kg/cm <sup>2</sup>	Displacement % %	k'	k' mean	k	Wave length $\lambda$ cm	$\frac{\lambda}{a}$
10	1.9	38	3.94	0.82	115,000	111,402	51		
11	1.9	38	3.73	0.73	109,500			3.62	1.9
12	1.8	36	4.17	0.956	110,800			3.62	2.0
13	1.7	34	4.82	1.06	110,300			3.38	1.99
14	1.5	30	5.17	1.225	95,400	Inelastic		2.75	1.85
15	1.6	32	4.83	0.59	101,400	tic		3.10	1.94
16	1.6	32	5.04	1.09	105,800	deformation		3.01	1.88

TABLE IV. Tests 17-26

Material, Celluloid  
 Modulus of elasticity,  $E = 23,500 \text{ kg/cm}^2$   
 Poisson's ratio,  $m = 2.45$   
 Plate thickness,  $h = 0.031 \text{ cm}$

Test No.	Plate width a cm	a/h	Wrinkling load s kg/cm <sup>2</sup>	Displacement % %	k'	k' mean	k	Wave length $\lambda$ cm	$\frac{\lambda}{a}$
17	1.9	61.3	1.01	0.45	121,300	119,200	52	3.73	1.96
18	1.8	58.1	1.075	0.406	116,900			3.53	1.96
19	1.7	54.9	1.235	0.365	119,900			3.16	1.86
20	1.5	48.4	1.57	0.602	118,900			2.97	1.97
21	1.4	45.2	1.86	0.642	118,400			2.59	1.85
22	1.3	42.0	2.14	0.3	121,600			2.45	1.80
23	1.2	38.7	2.42	0.918	117,200			2.38	1.98
24	1.1	35.5	2.95	1.05	119,700			2.22	2.00
25	1.0	32.2	3.36	1.26	112,300	Inelastic		2.15	2.15
26	0.8	25.8	3.78	1.65	72,100	deformation		1.61	2.01

TABLE V. Tests 27-36

Material, Celluloid									
Modulus of elasticity, $E = 15,800 \text{ kg/cm}^2$									
Poisson's ratio, $m = 2.415$									
Plate thickness, $h = 0.051 \text{ cm}$									
Test No.	Plate width a cm	a/h	Wrinkling load s kg/cm	Displacement %	$k'$	$k'$ mean	k	Wave length $\lambda$ cm	$\frac{\lambda}{a}$
27	1.25	24.6	5.85	1.595	68,900	In		2.44	1.955
28	1.3	25.5	5.34	1.295	68,000	elas-		2.52	1.94
29	1.35	23.6	5.08	1.125	69,800	tic		2.66	1.965
30	1.4	27.45	4.83	1.13	71,400	defor-		2.76	1.97
31	1.45	28.45	4.32	0.98	68,500	ma-		2.78	1.92
32	1.5	29.4	4.32	1.00	73,300	tion		2.93	1.95
33	1.6	31.4	4.07	0.99	79,300			3.17	1.98
34	1.7	33.3	3.61	0.847	80,400	78,300	49.3	3.38	1.99
35	1.8	35.3	3.16	0.722	77,300			3.48	1.94
36	1.9	37.25	2.80	0.60	76,200			3.8	2.00

b) Type of deformation.— Aside from the load which induces wrinkling, the type of deflection is of particular interest with respect to the wave length, for it enables us to decide where reinforcements are necessary.

We used a Zeiss instrument with which we practically calibrated the deformed plate.

Owing to the aforementioned irregular stress distribution near the free edges, we naturally expected some disturbance in the uniformity of the deflection. For that reason we had to ascertain the extent of the effect of the free edges on the deformation, because this boundary zone had to be eliminated before defining the wave length. In several specimens the first signs of wrinkles appeared at 1 to 1.5 a from the free edge. But by a very slight load increase the deformation spread

evenly over the entire strip. This undoubtedly is due to the slightly higher stress increase near the edges.

So in order to define this edge effect, we examined the boundary zone of a transparent strip of celluloid 0.05 cm thick and 1.9 cm wide after wrinkling. Our method consisted in determining the deformation as dissections perpendicular to the constrained edges. The dissections were 2 mm apart. The measuring points were 1 mm apart.

Since the shape of the lever made the measurement of the deformation on the constrained edge itself impossible, the ends of the dissections had to be determined afterward. The deformation over several wave lengths was measured 1.5 mm from the constrained edge on a line parallel to this edge. The middle lines between the tangents to the waves then yielded the position of the constrained edges, after which the contour lines, i.e., the lines of equal deflection from the plane, give us the deformation, shown on Figure 23.

The figures on the contour denote the deflection perpendicular to the median plane in 0.01 mm. The fourth half-wave already has exactly the same shape as the one following. The greatest deflection on the whole strip occurs on the free edge. The irregularities in the deformation do not extend beyond three half-waves.

So it may be stated that the effect of the free edge on the deformation does not exceed 1.5 times the width of the plate

from the free edge, and all waves outside of this defined boundary zone are included when defining the wave length.

However, since this does not preclude the possibility of any more extended edge effect under increasing deflection we determined the location of the zero deflection lines or of the junction lines for  $s = 4.83$ ,  $5.48$ , and  $5.93$  kg/cm at various degrees of deflection. The strip was 1.8 cm wide and 0.05 cm thick. But the test failed to show any difference in distance between two junction lines for these load stages, with the exception of their slope which, owing to the greater displacement of the constrained edges, was more pronounced (Fig. 24).

To follow the course of the wrinkles, we determined the deformation on the same plate for a half-wave, the results of which are plotted in Figures 25-27. At the left we find the deflection from the plane as dissection perpendicular to the constrained edges and the absolute values of the deflection; at the right, the deformation as contour. For  $s = 4.83$  kg/cm the deflection is perfectly elastic, while at higher loads part of the deflection is already of a permanent nature. From these deformations the disproportionate raise in wrinkling by small load increases, becomes apparent. The permanent deflection after releasing the load is shown as dissection and contour on Figure 28.

The wave length was defined by measuring the distance of maximum deflections from each other. The results of these

measurements are given in Tables II to V, with wave length  $\lambda$  in centimeters.

For  $\lambda/a$  we obtained the following figures:

Tests	1 - 9	$\lambda/a = 1.88 - 2.18$
	10 - 16	1.38 - 3.00
	17 - 26	1.35 - 3.15
	27 - 36	1.92 - 2.00

There is no difference in wave length for elastic or inelastic deflection as far as we could ascertain. The average  $\lambda/a = 1.97$ , as seen in Figure 29, shows  $\lambda/a$  plotted against  $\lambda/a$ .

c) Stress distribution at the beginning of wrinkling.— Here we attempted to determine the bending moments perpendicular and parallel to the constrained edges from the deflections developed in the plate after exceeding the wrinkling load. The plate was 0.05 cm thick, 1.8 cm wide, of celluloid No. 7, Table I; the measurements were made by  $s = 4.83$  kg/cm edge loading.

Our procedure was to approximate the dissections parallel and perpendicular to the constrained edges as arbitrary functions by a series of other given functions. Inasmuch as these dissections are valid as periodic functions, we chose the approximation by Fourier series. Then we transferred the measured values to a system of coordinates and plotted a smooth curve which followed the experimental points as closely as possible. This was followed by an harmonic analysis of empirical functions, after which we took a number of equidistant values from the curve. The individual periods were divided into twelve parts and the

coefficients of the sine and cosine terms of the Fourier series computed. Terms with coefficients, which in their order of magnitude went below the measuring accuracy of the Zeiss instruments, were disregarded in the second differentiation. From the quotient of the latter we determined the respective 12 ordinates which yield the values for  $\frac{\partial^2 w}{\partial x^2}$  and  $\frac{\partial^2 w}{\partial y^2}$ , that is, for the moments.

Table VI contains the perfectly elastic deflections perpendicular to the constrained edges.

The distribution of the computed moments

$$G_1 = -D \left( \frac{\partial^2 w}{\partial x^2} + \mu \frac{\partial^2 w}{\partial y^2} \right)$$

$$G_2 = -D \left( \frac{\partial^2 w}{\partial y^2} + \mu \frac{\partial^2 w}{\partial x^2} \right)$$

over a half-wave may be seen in Figures 30 and 31. The lines apply to  $G_1$  and  $G_2 = \text{constant}$ . The ascribed figures yield with  $-1.64 \times 10^{-3}$  as scale the moments  $G_1$  and  $G_2$  (kg/cm) and with  $-3.92$  the stress in the plate in kg/cm<sup>2</sup>. The maximum moments and stresses are in the center of the half-wave and amount to 0.469 and 0.325 kg/cm, and 112 and 78 kg/cm<sup>2</sup>.

It is seen that the plate stresses, due to wrinkling in bending, exceed the shear stresses of 96.6 kg/cm<sup>2</sup> at the edge soon after exceeding the buckling load. Because of the very pronounced increase in bending stress by further deflection, it becomes evident that a stress is quickly developed by the wrink-

les above the proportional elastic limit.

TABLE VI

Deflections in Dissections Perpendicular to the  
Constrained Edges in 1/1000 mm

	a <sub>s</sub>	b <sub>s</sub>	d	e <sub>s</sub>	g	h <sub>s</sub>	j	k <sub>s</sub>	m	n <sub>s</sub>	p
1	-13	-34	-66	-93	-117	-125	-138	-113	- 87	-49	-23
2	- 3	-13	-29	-51	- 76	-105	-125	-130	-116	-79	-25
3	20	23	37	21	4	- 37	- 68	- 95	-102	-76	-36
4	47	77	90	90	83	53	15	- 37	- 61	-60	-36
5	57	105	136	149	148	131	82	37	- 3	-27	-24
6	60	110	160	179	201	197	159	105	46	13	- 4
7	50	84	157	205	237	229	216	167	100	43	15
8	35	73	129	182	225	238	235	197	137	74	29
9	8	33	75	127	139	193	204	192	140	100	39
10	-11	-10	+35	74	119	163	186	184	155	106	45
11	-38	-45	-33	- 5	36	75	104	112	108	76	35
12	-49	-65	-72	-67	-33	0	50	52	57	45	22
13	-53	-73	-87	-96	-93	- 70	- 30	7	21	25	12

#### Tests with Duralumin

These experiments should be of special interest to the user of light metal. We used rolled plates 0.05 and 0.03 cm thick, alloy No. 681b, hardness 1/2. The elastic properties, modulus of elasticity, and Poisson's ratio were determined on samples taken from the same sheet; the modulus of elasticity varied between 748,000 and 775,000 kg/cm<sup>2</sup> (average: 760,000 kg/cm<sup>2</sup>); Poisson's ratio,  $m = 3.23$ .

The wrinkling tests were made with the aforementioned clamping device (Fig. 10). The effect of the edge loading on the displacement is graphed in Figure 32 (plate test No. 66). Tests 42, 44, 45, 48, 52-59, and 64-67 were made with the 0.03 cm

plates, and the load at wrinkling and the wave length determined. The data are shown in Table VII and Figure 33. The graph shows the transition from elastic to inelastic deflection between  $a/h = 53.3$  and  $33.3$ , and in conformity the  $k'$  values up to  $a/h = 53.5$  show a constant value of about 3,490,000. The figures for  $k$  range between 51.1 and 47.6; the average is 49.2. Below  $a/h = 53.3$  the  $k'$  values continue to decrease to 1,940,000.

The experiments (Nos. 43, 46, 49-51, and 60-63) with the 0.05-centimeter plates are included in Table VII, and Figure 34 denotes the effect of  $a/h$  on the collapsing load. The transition from elastic to inelastic deflection occurs between  $a/h = 56$  and  $40$ . The  $k'$  values are again practically constant, ranging between 3,740,000 and 3,500,000.  $k$  averaged 51.0, a figure only slightly different from the previously obtained value.

Figure 35 exhibits the  $\lambda/a$  values for tests 42-67, plotted against plate width  $a$ . The  $a/h$  ratio fluctuated between 116.8 and 33.3, and the ratio of wave length to plate width between (1.68) 1.89 and 2.02. The average for  $\lambda/a$  for all tests with duralumin plates was  $\lambda/a = 1.97$ .

TABLE VII. Tests 42-67

Material, Duralumin  
 Modulus of elasticity,  $E = 760,000 \text{ kg/cm}^2$   
 Poisson's ratio,  $m = 3.23$

Test No.	Dimensions width a cm	thick- ness h	a/h	Wrink- ling load s kg/cm	$k'$	k	Wave length $\lambda$ cm	$\frac{\lambda}{a}$
42	2.00	0.03	66.6	24.6	3,620,000	50.9	3.92	1.96
43	2.00	0.05	40	93	2,676,000	(41.8)	3.96	1.98
44	1.60	0.03	53.3	35.8	3,394,000	47.7	3.17	1.98
45	2.80	0.03	93.3	12.1	3,513,000	49.4	5.56	1.985
46	2.80	0.05	56	56.4	3,537,500	49.8	5.75	2.05
48	2.80	0.03	93.3	12.2	3,543,000	49.9	5.55	1.98
49	2.00	0.05	40	96	3,072,000	(43.2)	3.95	1.975
50	1.60	0.05	32	98	2,007,000	(28.3)	3.18	1.985
51	1.60	0.05	32	103	2,110,000	29.7	3.10	1.940
52	2.80	0.03	93.3	11.8	3,426,000	48.2	5.50	1.960
53	2.80	0.03	93.3	12.5	3,360,000	51.1	5.45	1.945
54	2.00	0.03	66.6	24.4	3,615,000	50.8	3.80	1.90
55	2.00	0.03	66.6	24.3	3,600,000	50.6	4.05	2.02
56	1.60	0.03	53.3	36.7	3,480,000	49.0	3.10	1.94
57	1.60	0.03	53.3	35.7	3,385,000	47.6	3.18	1.99
58	1.00	0.03	33.3	52.5	1,940,000	(27.3)	2.00	2.00
59	1.00	0.03	33.3	59.5	2,204,000	(31.1)	1.89	1.89
60	2.80	0.05	56	57.5	3,746,000	52.7	5.39	1.91
61	2.80	0.05	56	55.5	3,501,000	49.6	5.47	1.95
62	3.50	0.05	70	37	3,626,000	51.0	7.15	1.98
63	3.50	0.05	70	39	3,822,000	53.7	7.05	1.96
64	3.50	0.03	116.8	7.8	3,547,000	49.9	7.20	2.00
65	3.50	0.03	116.8	7.2	3,267,000	46.0	6.83	1.95
66	1.60	0.03	53.3	40	3,792,000	53.3	2.79	1.68
67	1.00	0.03	33.3	55	2,036,000	(28.6)	1.98	1.98

TABLE VIII. Tests 68-80, 87, 88

Material, Brass  
 Modulus of elasticity,  $E = 943,000 \text{ kg/cm}^2$   
 Poisson's ratio,  $m = 3.06$   
 Plate thickness,  $h = 0.02 \text{ cm}$

Test No.	Plate width a cm	a/h	Wrinkling load s kg/cm	$k'$	k	Wave length $\lambda$ cm	$\frac{\lambda}{a}$
68	2.0	100	8.45	4,225,000	48.0	4.35	2.15
69	2.0	100	8.26	4,130,000	47.0	3.80	1.9
70	2.8	140	4.54	4,449,000	50.6	5.46	1.95
71	2.8	140	4.54	4,449,000	50.6	5.43	1.95
72	1.6	80	13.7	4,384,000	49.9	3.17	1.98
73	1.6	80	13.5	4,320,000	49.1	3.38	2.11
74	0.8	40	31.8	2,544,000	28.9	1.54	1.93
75	1.0	50				1.97	1.97
76	1.2	60				2.25	1.88
77	2.0	100	8.45	4,225,000	48.1	4.08	2.05
78	2.8	140	4.43	4,341,000	49.4	5.38	1.93
79	1.0	50	23.0	2,875,000	32.7	1.90	1.90
80	1.0	50	22.9	2,863,000	32.6	1.82	1.82
87	3.5	175	3.16	4,933,550	56.1	7.52	2.14
88	3.5	175	2.96	4,625,000	52.6	6.3	1.8

## Experiments with Brass Plates

The samples were 0.02 cm thick rolled brass. Tensile tests made on six specimens yielded  $E = 943,000 \text{ kg/cm}^2$  and transverse elongation  $m = 3.06$ .

The results of the deflection tests are given in Table VIII and Figure 36. As long as  $k'$  remains constant by  $a/h \geq 70$ , the deflection is elastic (tests 68-73, 77, 78, 87, 88). When  $a/h < 70$ , formula (23) is inapplicable to this material;  $k'$  becomes smaller, so that by  $a/h = 40$  it has dropped to 2,544,000. For elastic deflection  $k = 48.0 - 56.1$ ; the average

is  $k = 50.1$ .

The ratio of wave length to plate width  $\lambda/a$ , remains practically constant and raises between 1.8 and 2.15. The average of all tests is 1.96. In Figure 37, where  $\lambda/a$  is plotted against the plate width, the individual  $\lambda/a$  figures are in close agreement with the mean values shown as dotted line.

### C o n c l u s i o n

Owing to the high elastic deformability of celluloid, it was not only possible to observe the beginning but also to ascertain the type of deflection. The test data on celluloid were affirmed by the experiments with duralumin and brass.

According to our experiments the load at wrinkling can be accurately expressed by the formula  $s = k \frac{D}{a^3}$  ( $k = 49$  to  $50$ ), as set up from experiments with celluloid and substantiated by those on duralumin and brass. Its limit of applicability is the proportional elastic limit.

In wrinkling, two cases must be distinguished: deflection prior to reaching yield limit (elastic deflection); and deflection after the yield limit has been reached (inelastic deflection). The transition from elastic to inelastic deflection in the individual materials is characterized by a certain ratio of plate width to plate thickness  $a/h$ , which for celluloid is 34, for duralumin, 50, and for brass, 70. The greater the elastic deflection in the material, the lower the  $a/h$  ratio of transition. In contrast to Southwell and Skan, our figures for the

wrinkling loads were about 43% lower. This discrepancy finally becomes greater than we expected from the previously stated effect of inexact edge constraint. Then the shape of the deflection surely has some effect also. According to Southwell, the wave lengths should equal 1.6 times the plate width, but our tests yielded 1.97  $\lambda/a$  in every case. Timoschenko's figures are slightly higher, although it should be remembered that in his tests all four edges were supported.

Regarding the deflection itself, the following may be stated: Once a certain load - the wrinkling load - has been exceeded, the equilibrium between the internal and external stresses ceases to be certain. The beginning of instability is accompanied by a formation of regular, wavelike wrinkles. Near the free edge the uniformity is interrupted by the uneven stresses prevailing at that point. The deflection at the free edge is approximately 15% greater than in the plate center. The wave length of the deflection is in a constant ratio to the plate width,  $\lambda/a = 1.97$ , and is unaffected by the plate thickness and the material.

Translation by J. Vanier,  
National Advisory Committee  
for Aeronautics.

## R e f e r e n c e s

1. Andrade, E. M. da C. : The Distribution of Slide in a Right Six-Face Subject to Pure Shear. Proc. Roy. Soc. Series A, Vol. 85, 1911, p. 448.
2. Bryan, G. H. : On the Stability of a Plane Plate under Thrusts in its Own Plane, with Applications to the "Buckling" of the Sides of a Ship. Proc. of the London Math. Soc., Vol. 22, 1891, p. 54.
3. Engesser, Fr. : Über die Knickfestigkeit gerader Stäbe. Zeitschr. d. Hann. Ing.- und Arch.-Vereins, Vol. 35, 1889, p. 455.
4. Engesser, Fr. : (Berichtigung zu Schr. 3) Schweizer Bauzeitung, Vol. 26, p. 24.
5. Coker, E. G. : Optical Determination of the Variation of Stresses in a Thin Rectangular Plate Subjected to Shear. Proc. Roy. Soc., Series A, Vol. 86, 1911, pp. 291-319.
6. Filon, L. N. G. : On an Approximate Solution for the Bending of a Beam of a Rectangular Cross Section under any System of Load, with Optical Reference to Points of Concentrated or Discontinuous Loading. Phil. Trans., Series A, Vol. 201, 1903, p. 126.
7. Inglis, E. : Stress Distribution in a Rectangular Plate Having Two Opposing Edges Sheared in Opposite Directions. Proc. Roy. Soc. Series A, Vol. 103.
8. Karman, Th. v. : Untersuchungen über Knickfestigkeit. Mitteilungen über Forschungsarbeiten, No. 81, 1910.

9. Lamarle, : Memoires sur la Flexion du Bois, 1845.
10. Lilly, W. E. : Journal Junior Inst. Eng., Vol. 18, 1907, pp. 72-181.
11. Lilly, W. E. : Web Stresses in Plate Girders and Columns. Engineering, Feb. 1, 1907, pp. 136-139.
12. Lilly, W. E. : The Design of Plate Girders and Columns. Engineering, 1908.
13. Love, : Lehrbuch der Elastizität. Deutsch von A. Timpe, Chap. 22, 1907.
14. Lord Rayleigh, : The Theory of Sound. 1894, Vol. 1 & 2.
15. Ritz, W. : Über eine neue Methode zur Lösung gewisser Variationsprobleme der mathematischen Physik Journal f. d. reine und angew. Mathematik. Vol. 135, 1909, p. 1 (s. auch seine gesammelten Werke, Paris, 1911).
16. Runge, C. and König, H. : Vorlesungen über numerisches Rechnen, Berlin, 1924, pp. 189-237.
17. Schwerin, E. : Die Torsionsstabilität des dünnwandigen Rohres. Zeitschr. f. angew. Math. u. Mech., Vol. 5, No. 3, p. 325.
18. Southwell, R. V. and Skan, Sylvia W. : On the Stability under Shearing Forces of a Flat Elastic Strip. Proc. Roy. Soc., Series A, Vol. 105.
19. Southwell, R. V. and Skan, Sylvia W. : Note on the Stability Under Shearing Forces of a Flat Elastic Strip and an Analogy with the Problem of a Laminar Fluid Motion. Proc. of the First Intern. Congr. for Appl. Mech., Delft, 1924, p. 326.

30. Tetmajer, L. v. : Die angewandte Elastizitäts- und Festigkeitslehre. pp. 378-405. Leipzig and Vienna. 3d ed.
31. Timoschenko, S. : Über die Stabilität elastischer Systeme. Kiew, 1910.
32. Timoschenko, S. : Über die Stabilität versteifter Platten. Der Eisenbau, Vol. 12, 1921, pp. 147-163.

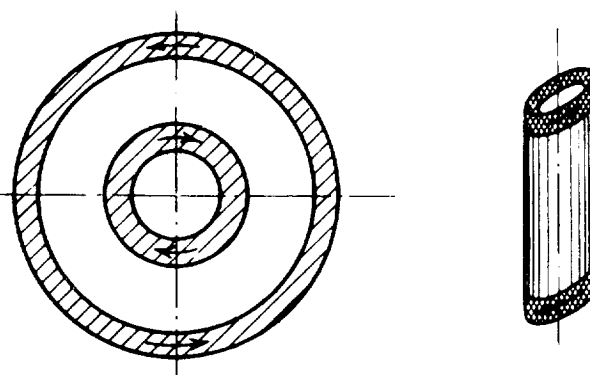


Fig. 1 Circular ring and tube stressed in shear.

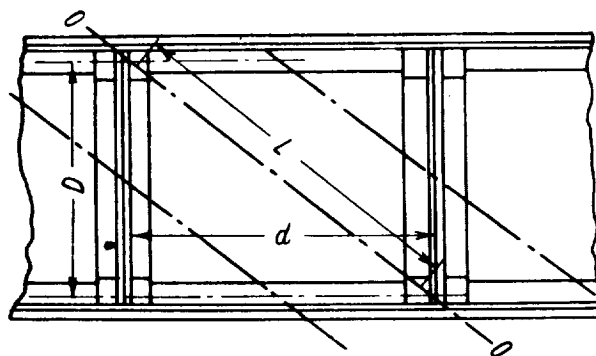


Fig. 3 Panel between two stiffeners (Lilly).

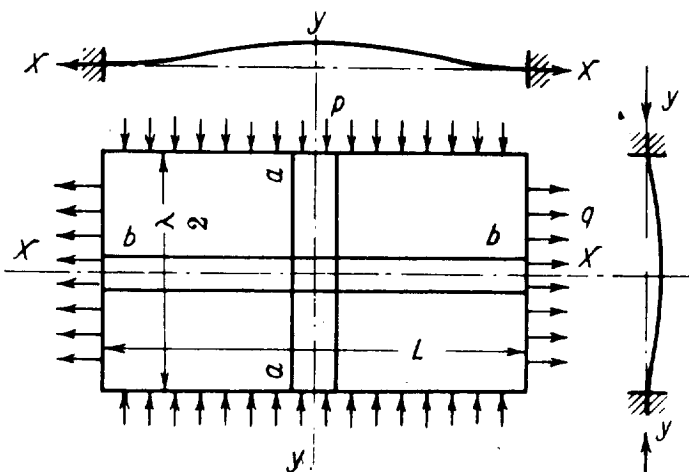


Fig. 4 Forces acting on a plate element (Lilly).

Section C-D

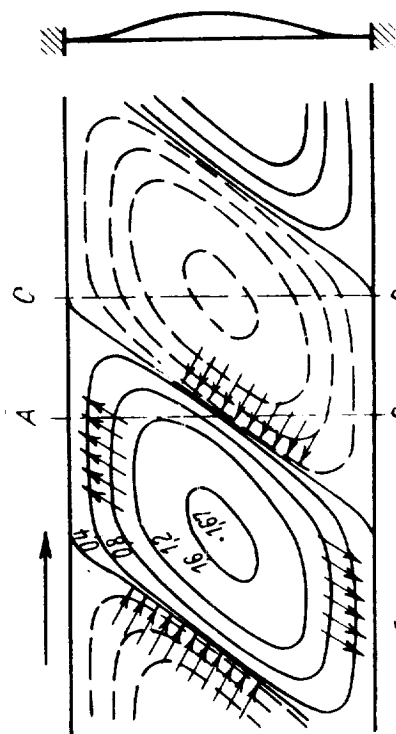


Fig. 2 Wrinkling due to shear on a flat plate. (Contours according to Southwell & Skan).

Section A-B

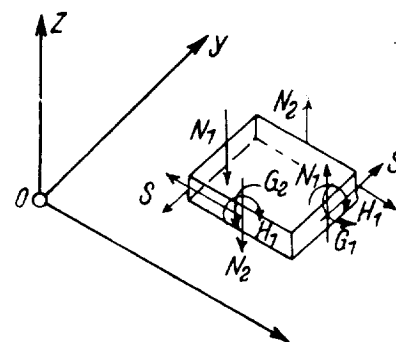


Fig. 7 Plate element with applied moments and resultant stresses.



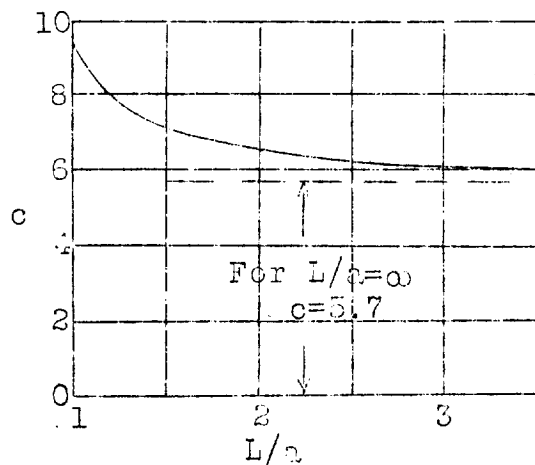


Fig. 5 Wrinkling loads  
(Timoschenko)

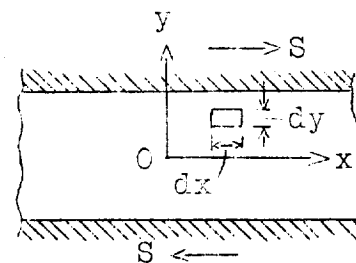


Fig. 6 Plate element  
(Southwell & Skan)

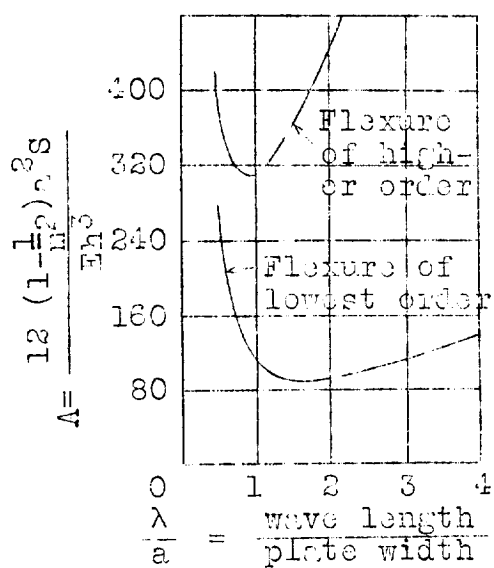


Fig. 8 Wrinkling loads  
(Southwell & Skan)

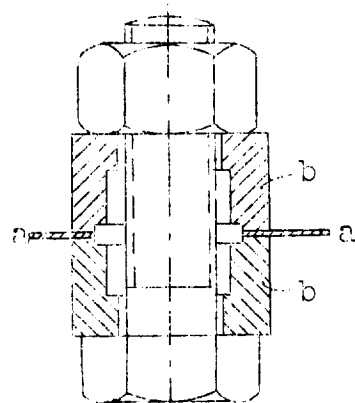


Fig. 9 Cut through  
clamps and  
test strips.



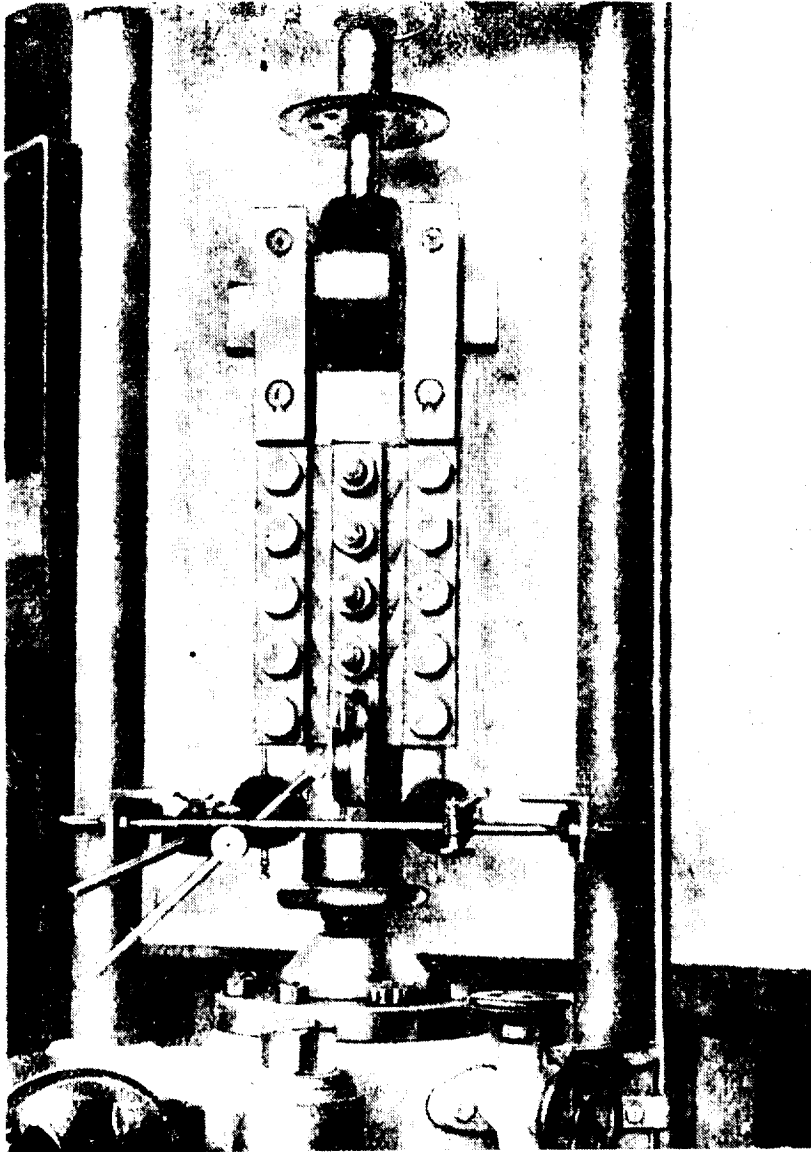


Fig. 10  
Test  
arrangement  
(vertical).

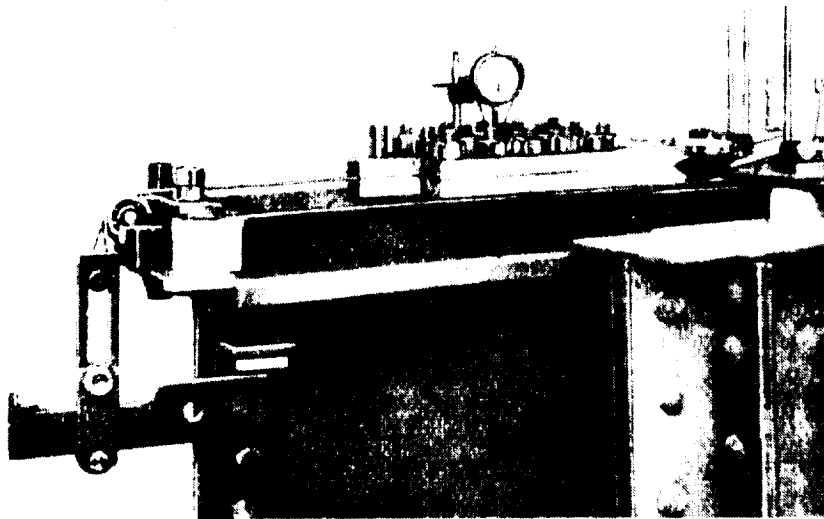


Fig. 11  
Test  
arrangement  
(horizontal)



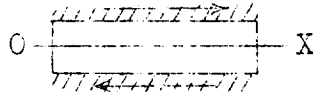


Fig. 12 Plate according to Coker

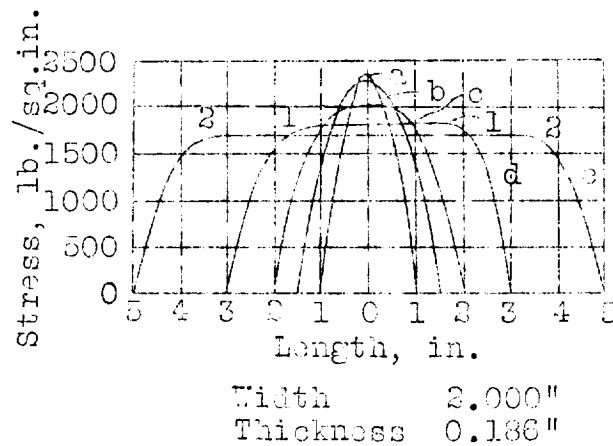


Fig. 13 Shear stress distributed over square plate (Coker)

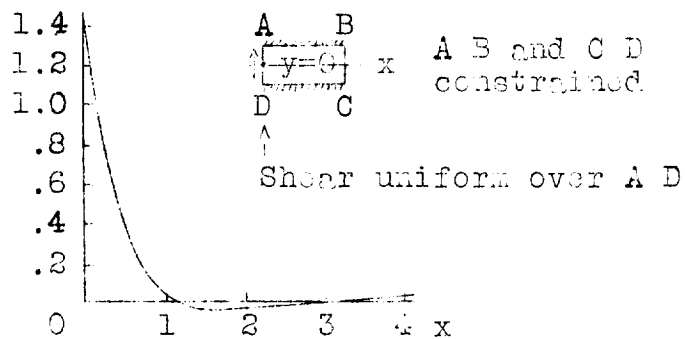


Fig. 14 Distribution of shear stress along center line 0-x



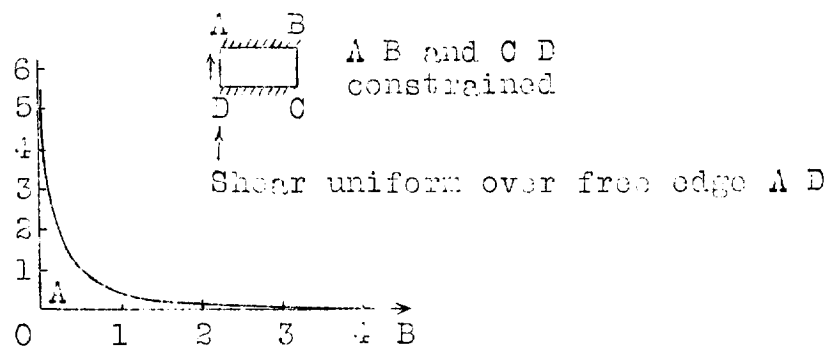


Fig. 15 Stress perpendicular to edge  $y=1$

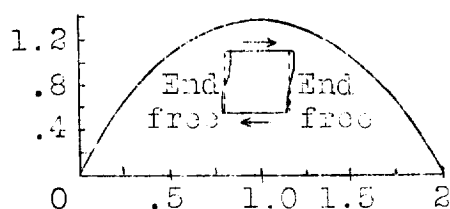


Fig. 16 Shear stress along center line for a square plate

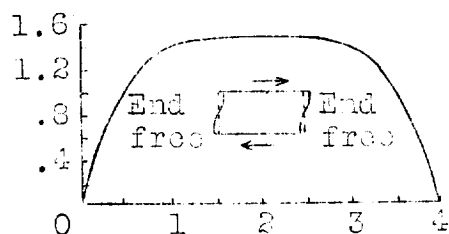


Fig. 17 Shear stress along center line for a plate with, long side/short side = 2 ratio

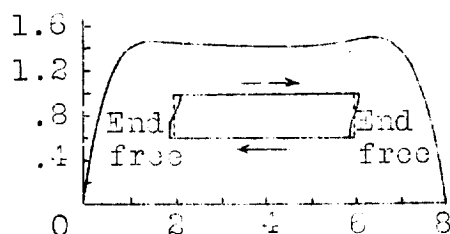


Fig. 18 Shear stress along center line for a plate with, long side/short side = 4 ratio



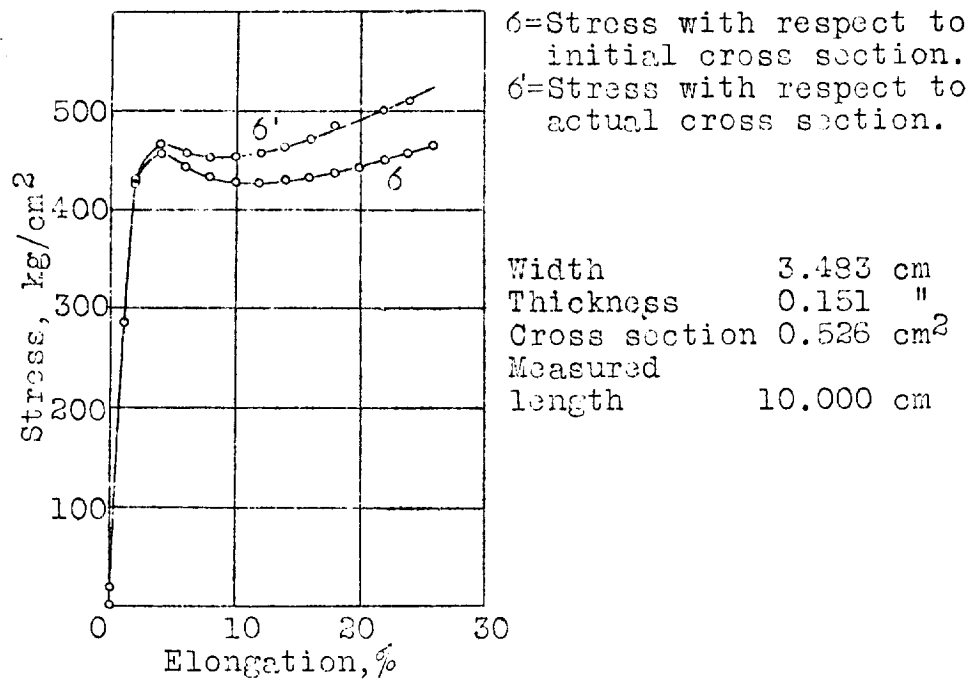


Fig. 19 Tension test on celluloid.

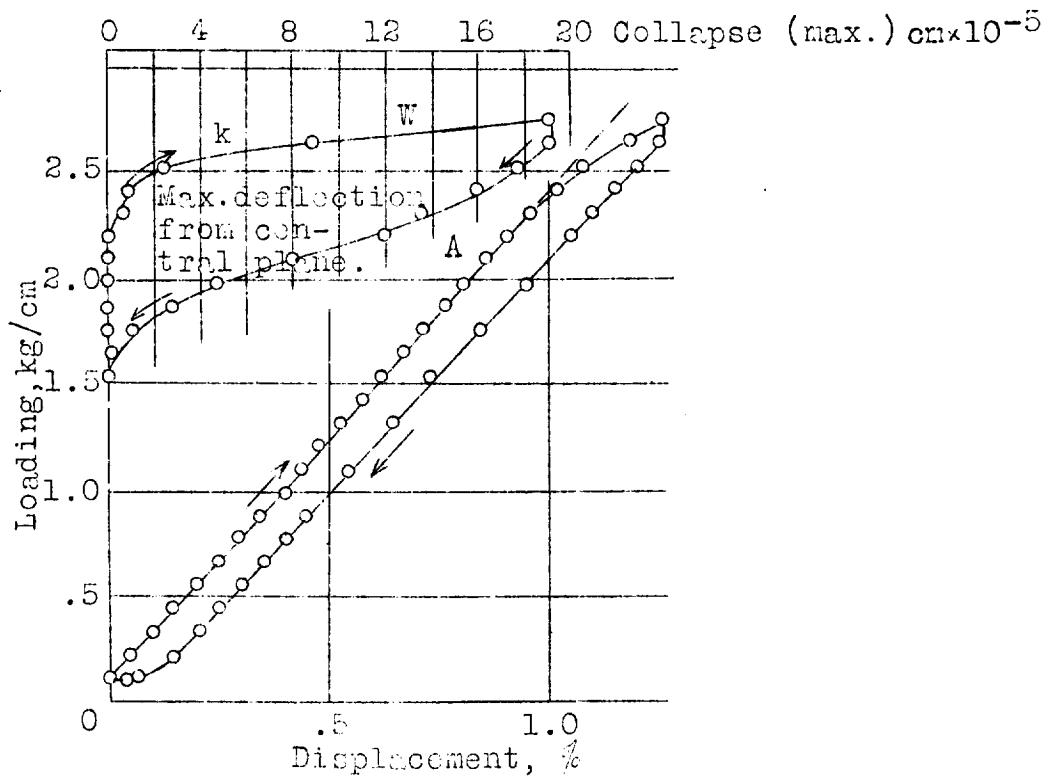


Fig. 20 Wrinkling test of celluloid elastic deflection.



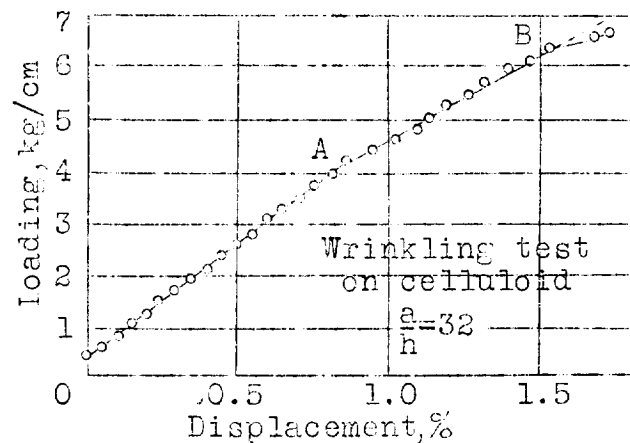


Fig. 21 Wrinkling test on celluloid, inelastic deflection.

—○— Test No. 1-9  
 —+— " " 10-16  
 —x— " " 17-26  
 —△— " " 27-36

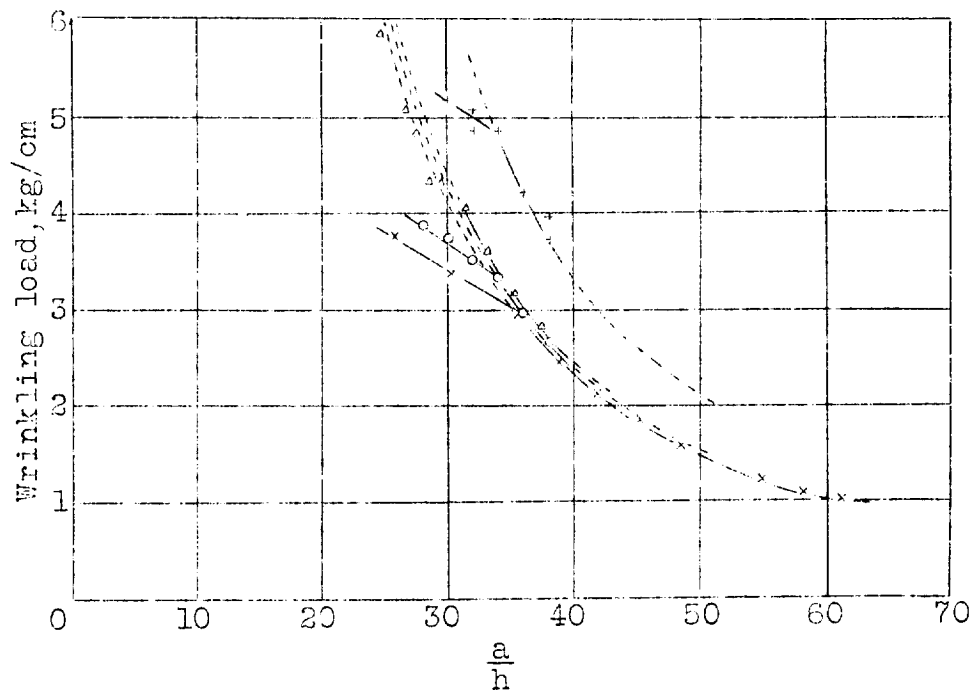


Fig. 22 Wrinkling loads according to tests on celluloid.



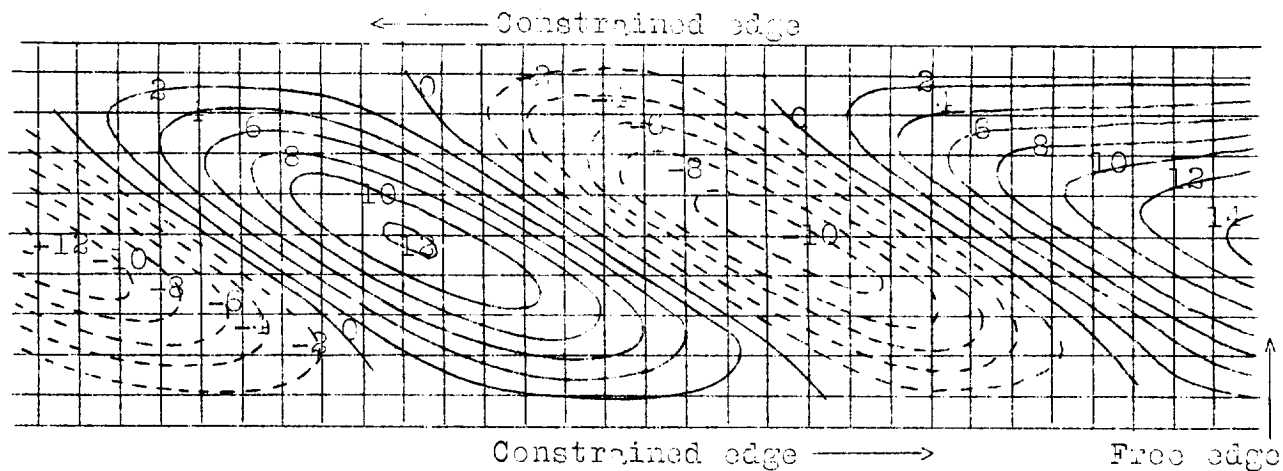


Fig. 23 Deformation on free edge, scale;  $\text{mm} \times 10^{-3}$

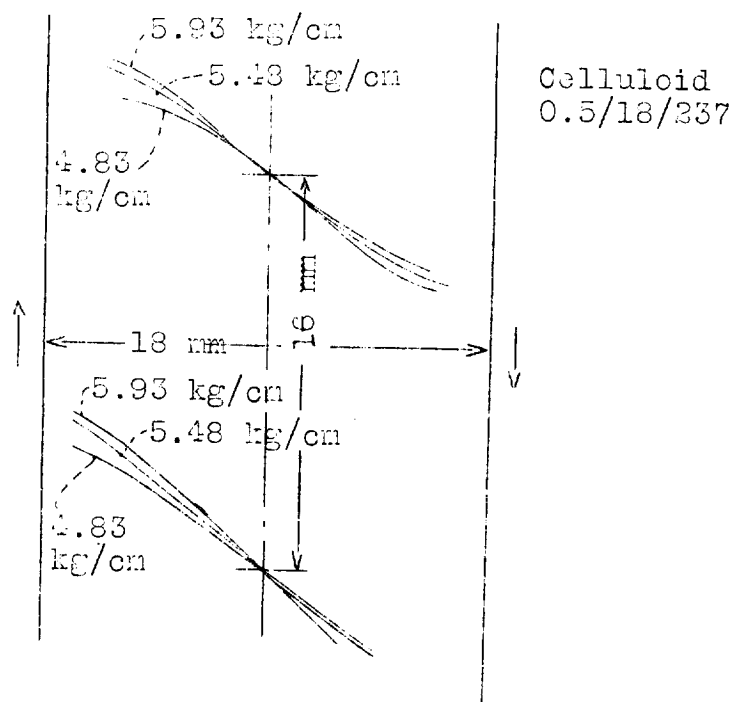


Fig. 24 Location of junction lines for various edge loadings.



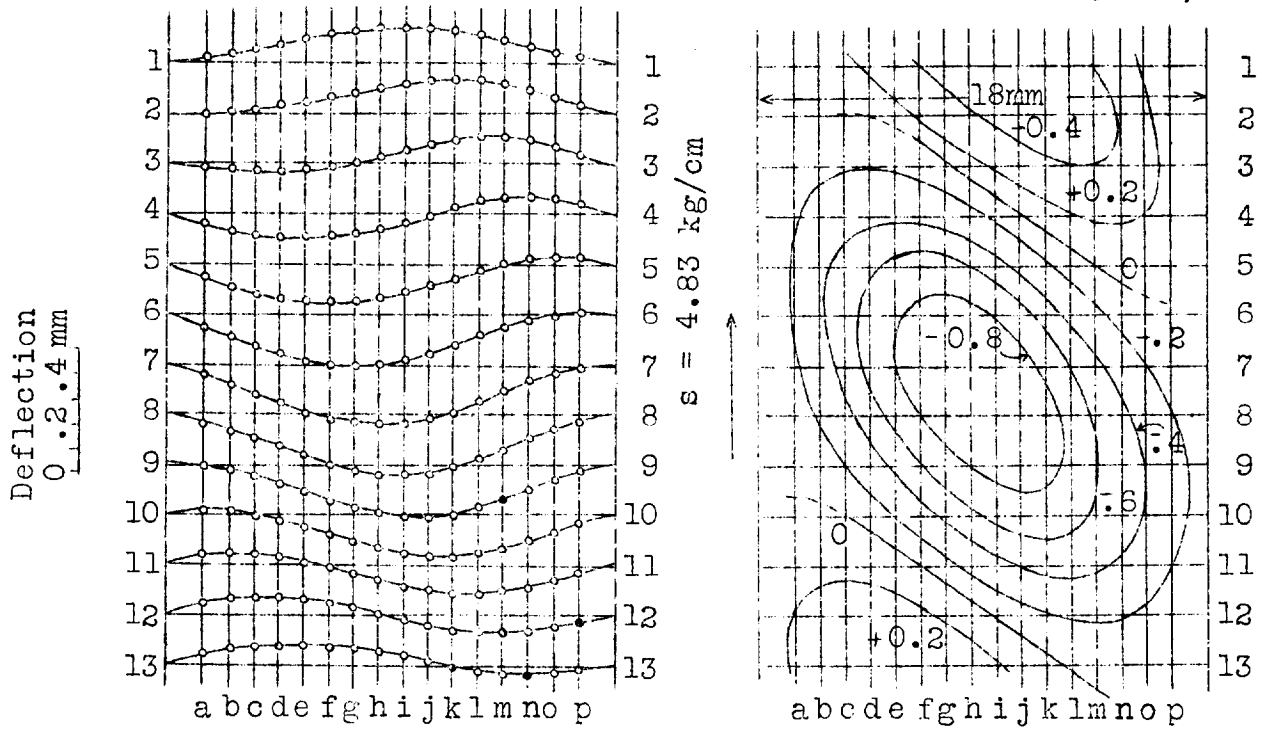


Fig.25 Wrinkling by,  $s = 4.83$  kg/cm, edge loading.

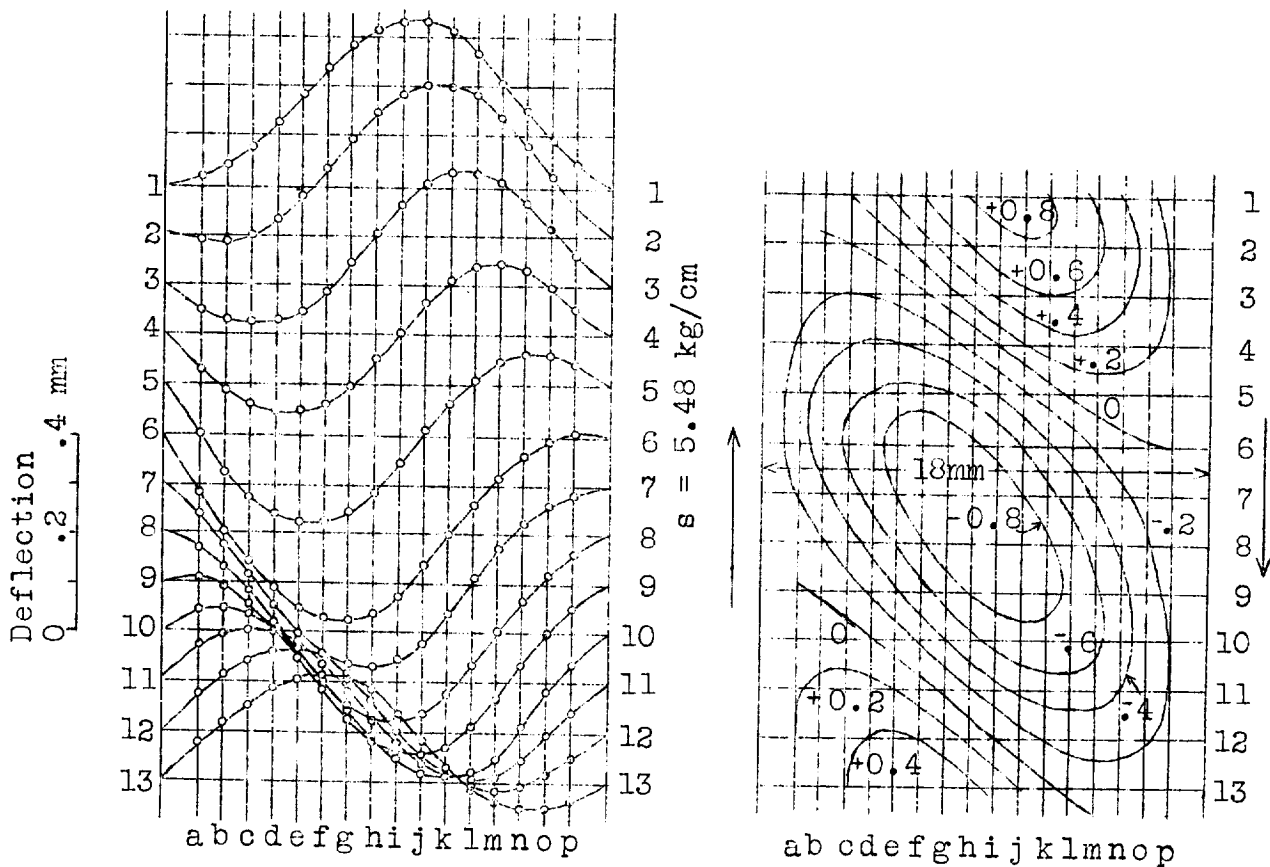


Fig.26 Wrinkling by,  $s = 5.48$  kg/cm, edge loading.



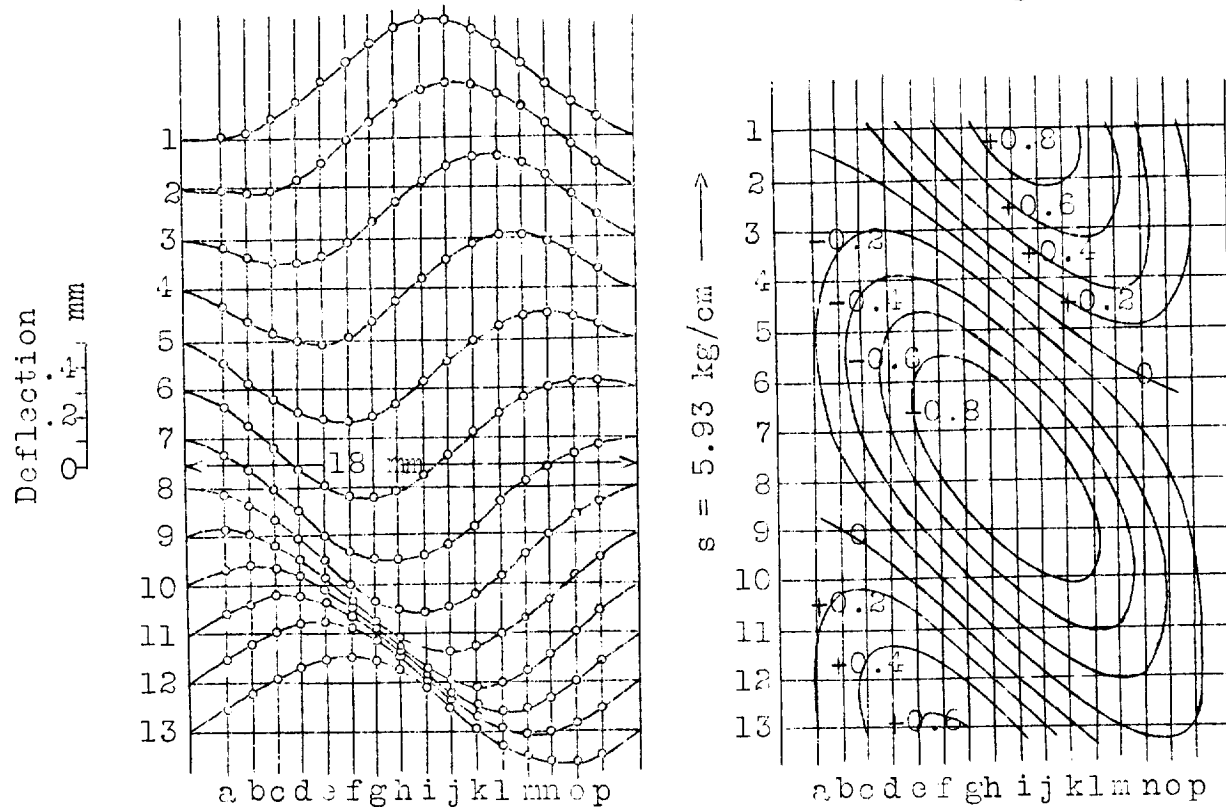


Fig.27 Wrinkling by edge loading,  $s = 5.93 \text{ kg/cm}$

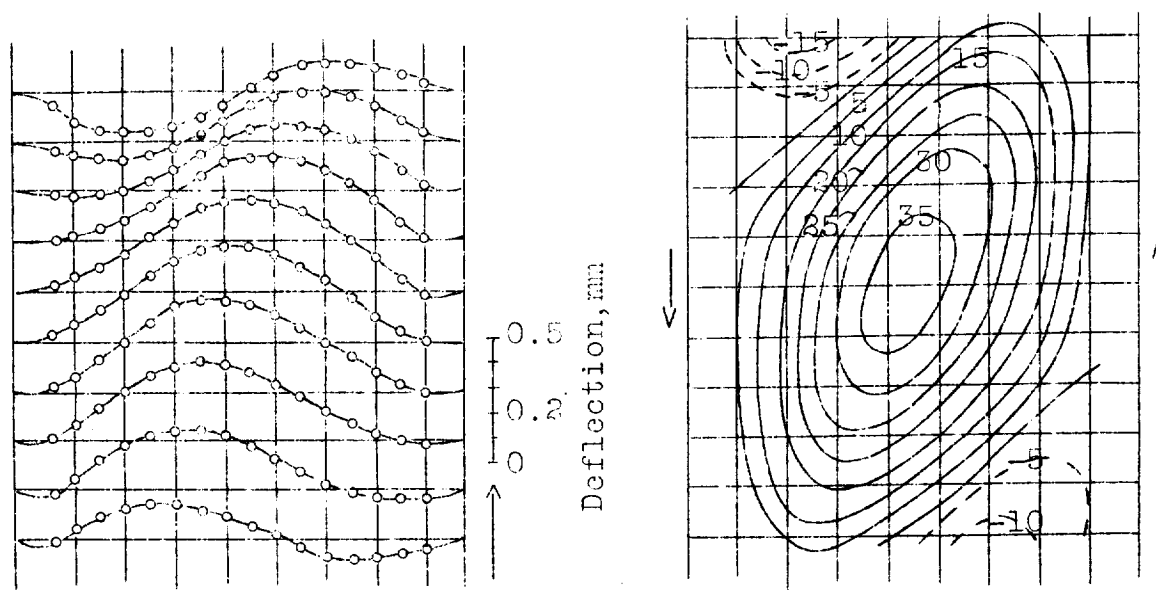


Fig.28 Permanent deformation in 0.05x1.79 cm plate.



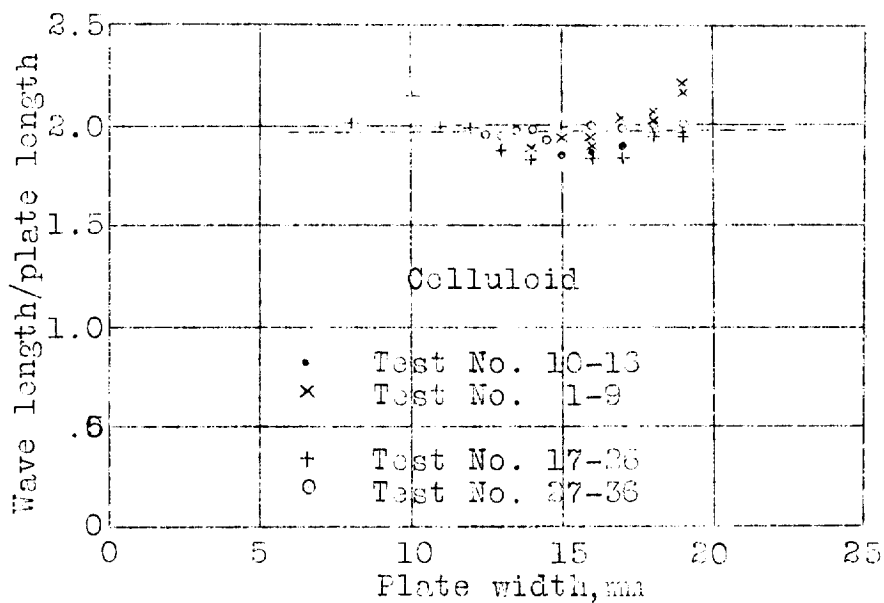


Fig. 29 Wave length plotted against plate width.

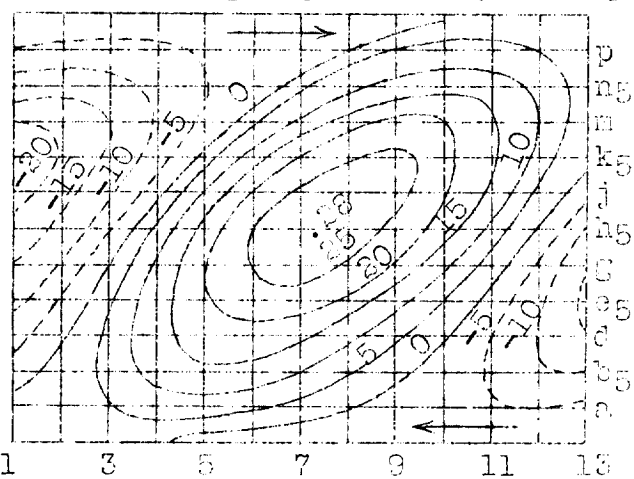


Fig. 30 Distribution of bending moments.  $G_1$

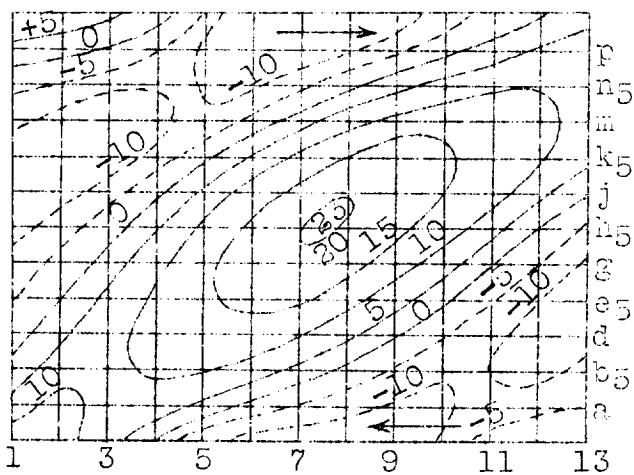


Fig. 31 Distribution of bending moments.  $G_2$



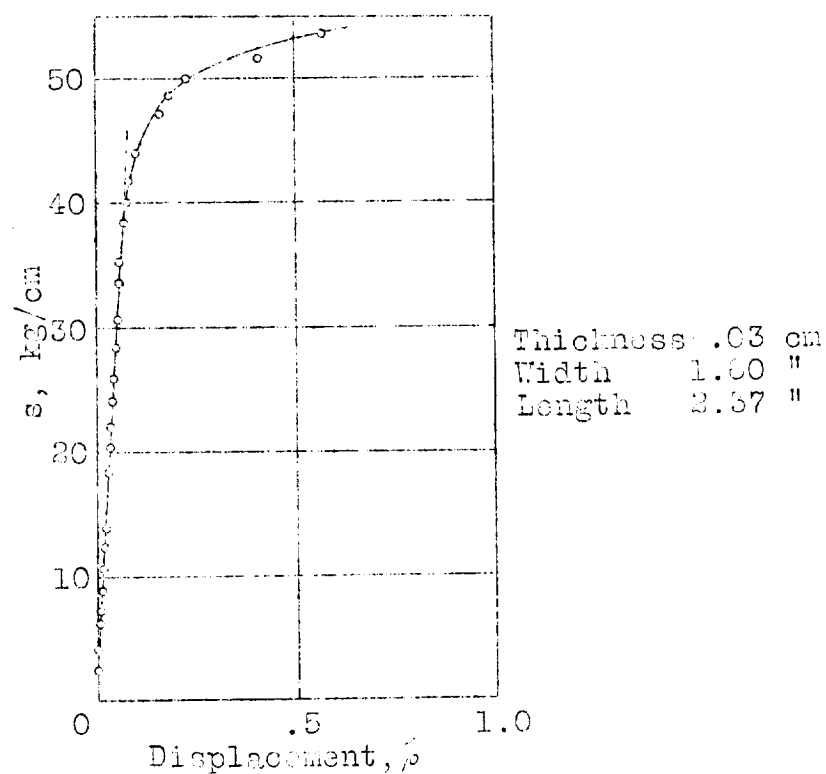


Fig. 32 Wrinkling test on duralumin plate.

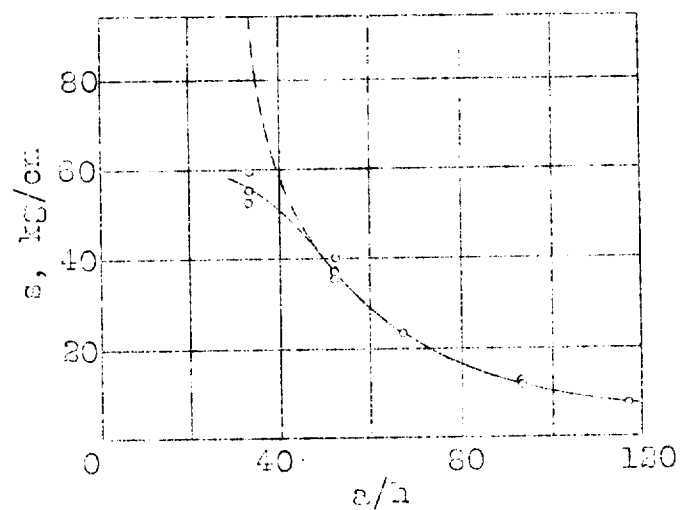


Fig. 33 Wrinkling loads for duralumin.



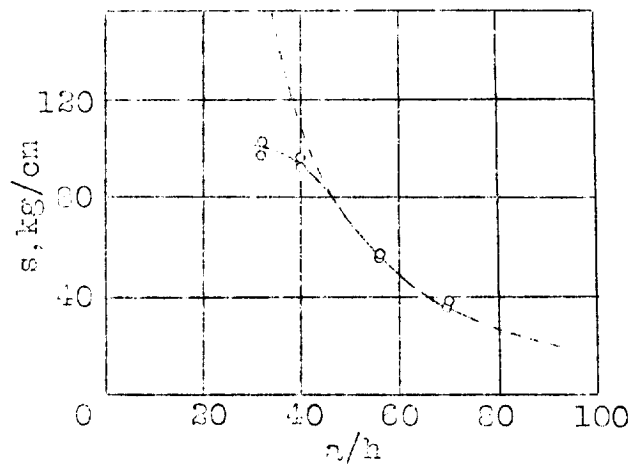


Fig. 34 Wrinkling loads for duralumin

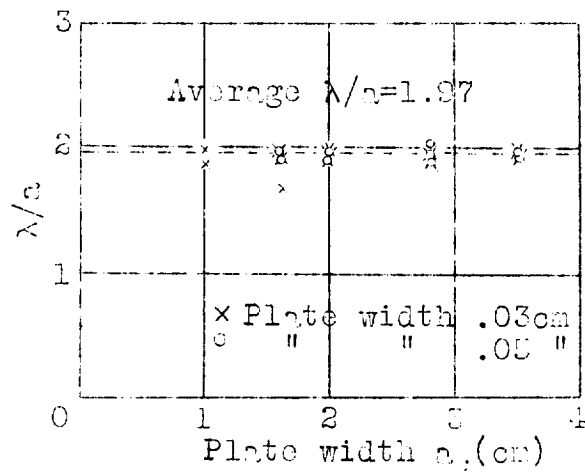


Fig. 35 Wave length for duralumin



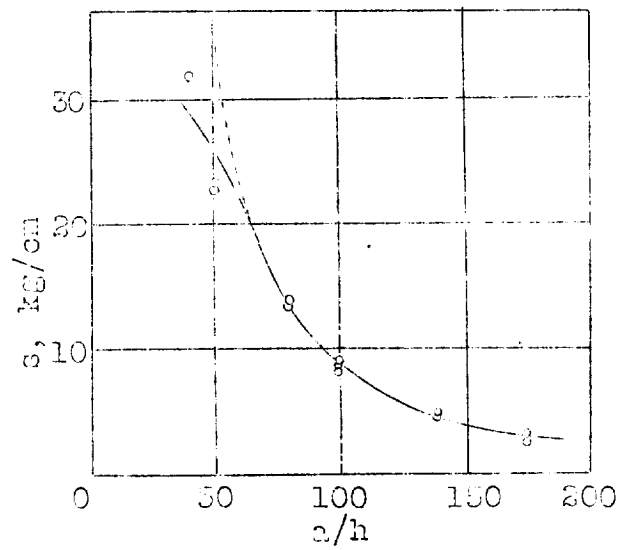


Fig. 36 Wrinkling loads for brass

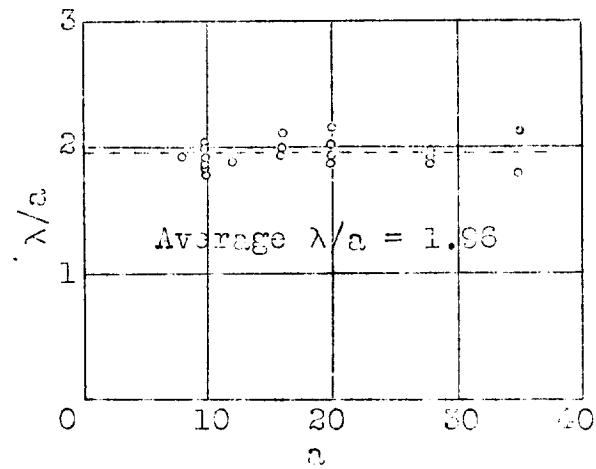


Fig. 37 Wave length for brass

